A Note on the Use of the Second Vertical Derivative (SVD) of Gravity Data with Reference to Indonesian Cases

Prihadi Sumintadireja[1], Darharta Dahrin[2] & Hendra Grandis[2]*

[1]Faculty of Earth Science and Technology, Institut Teknologi Bandung,
Jalan Ganesha 10, Bandung 40132, Indonesia
[2]Faculty of Mining and Petroleum Engineering, Institut Teknologi Bandung,
Jalan Ganesha 10, Bandung 40132, Indonesia
*E-mail: grandis@geoph.itb.ac.id

Abstract. Gravity data analysis and interpretation are based, among others, on their spatial variation represented by horizontal and vertical gradients. The gradient or derivative of a gravity field can be calculated either in the spatial domain or the wave-number domain. Historically, the second vertical derivative (SVD) of gravity data can be used to delineate the boundaries of anomalous sources. This paper addresses inappropriate use of the SVD of gravity data, with reference to current practices in Indonesia. The SVD's relative magnitude along a profile is widely used to define whether a density contrast and its dipping orientation correspond to a normal or reverse fault, which may be geologically incorrect. Furthermore, the SVD is calculated by approximation using the horizontal derivative, which may be erroneous especially with poorly distributed data and anomalous 3D sources. We exemplify our analysis with synthetic data and propose a more appropriate spectral-based analysis using field data.

Keywords: *anomaly enhancement; basin delineation; fault; gradient; potential field.*

1 Introduction

Potential field (gravity and magnetic) methods are used on a wide variety of scales, i.e. from basin delineation at a regional scale to prospect investigation at a very detailed scale. Spatial derivatives of potential field data are commonly analyzed for qualitative and semi-quantitative interpretation. Horizontal and vertical gradients are expected to enhance anomalous source boundaries from anomaly maps [1,2]. On the other hand, decaying characteristics of the anomaly may be used to infer the lateral position and depth of simple or elementary anomalous sources, as in Euler deconvolution or its variants [3,4].

The Fourier domain is often preferred for advanced processing of gravity and magnetic data, mostly because of speed and simplicity in operation, especially with the vast amounts of data acquired in recent years. However, with the advances of computational tools, grid-based data processing in the spatial domain can also be efficiently executed. The choice of the calculation technique

Received December 7th, 2017, Revised March 27th, 2018, Accepted for publication March 29th, 2018.
 ISSN: 2337-5779, DOI: 10.5614/j.eng.technol.sci.2018.50.1.9

is more or less determined by the characteristics of the intended result [1,5].

Second vertical derivative (SVD) analysis has been used as a tool for delineation of anomalies since the early 1950s due to its effectiveness in enhancing gravity data that otherwise appear very smooth. The calculation is performed manually by using a predefined template in the spatial domain, e.g. the so-called Elkins and Baranov methods [6,7]. In Indonesia, SVD analysis of gravity data is widely employed to delineate sedimentary basins in hydrocarbon exploration [8], to map faults in geothermal exploration [9], and in geological studies in general [10,11]. However, lack of awareness of the fundamental concepts and lack of effort in finding available computational resources lead to doubtful practices of which the results are unreliable. For example, the SVD is usually approximated by the second horizontal derivative along a profile of gravity data, mostly with poor resolution. Furthermore, the SVD is often directly used to infer geological structures, more particularly normal or reverse faults [9-11], which may be geologically incorrect. This paper addresses the misconception and improper use of the SVD technique and contains some remarks for the proper application of SVD analysis and its limitations.

2 Second Vertical Derivative (SVD) of Gravity

The calculation of gradients is intended to enhance subtle features of gravity data that are otherwise not visually noticeable from the original data. High gradients can be associated with a high contrast of physical properties of the subsurface and vice-versa. Gradients, and also their magnitude, are usually employed to delineate boundaries of anomalous sources. The SVD of the vertical component of gravity, g_z, can be calculated in the spatial domain from the horizontal gradients by using the Laplace's Eq. in Eq. (1) [1,5]:

$$\frac{\partial^2 g_z}{\partial z^2} = -\left(\frac{\partial^2 g_z}{\partial x^2} + \frac{\partial^2 g_z}{\partial y^2} \right) \tag{1}$$

For an elongated anomaly along the *y*-axis, the SVD can be approximated by the second horizontal derivative of the gravity data along the *x*-axis in Eq. (2):

$$\frac{\partial^2 g_z}{\partial z^2} \approx -\frac{\partial^2 g_z}{\partial x^2} \tag{2}$$

In the wave-number domain, or Fourier domain, the SVD is usually calculated by using the following Eq. (3) [5,12]:

$$\frac{\partial^2 g_z}{\partial z^2} = F^{-1}\left(|\mathbf{k}|^2 G_z \right) \quad \text{with} \quad |\mathbf{k}|^2 = k_x^2 + k_y^2 \tag{3}$$

where G_z is the Fourier transform of g_z, k_x and k_y are wave numbers on the x- and y-axis respectively, while F^{-1} is the inverse Fourier transform operator.

In general, derivatives in all coordinate directions can be calculated in the wave-number domain using 2D fast Fourier transform (FFT). The derivatives enhance high-frequency components contained in the data, as clearly indicated by Eq. (3), i.e. multiplication by the wave number with the derivative order as the exponent. Therefore, derivative maps from gravity data appear to be 'noisy' compared to their original data [12,13]. In the subsequent parts of this paper, all derivative calculations were done in the spatial domain to minimize the high-frequency amplification effect of the wave-number processing [1]. In addition, we intend to exemplify the utility of freely available software if 2D frequency domain analysis tools are not available [14].

3 Bott's Criteria for Interpreting the SVD

Historically, the ability of the SVD to delineate anomalous source boundaries has attracted practitioners since the early 1950s using virtually manual procedures [6,7]. Within the perspective of 1D approximation, Bott [15,16] proposed simple criteria for interpreting a negative gravity anomaly based on the relative magnitude of the SVD or $|g''|$ along a profile. When $|g''_{max}|$ is greater than $|g''_{min}|$ then the anomaly corresponds to a sedimentary basin with inward sloping edges, while if $|g''_{max}|$ is smaller than $|g''_{min}|$ then the anomalous source is a granite pluton with outward sloping edges.

To illustrate features enhanced by SVD and to verify Bott's criteria, we use 3D synthetic models with edges that slope inwards and outwards for a basin and pluton respectively with 3 km thickness and a density contrast of -0.5 gr/cm^3. The model blocks cover a volume of 30 x 30 x 40 km^3 discretized into cubes with 0.1 km edges to represent the dipping sides of the models smoothly. The 3D gravity forward modeling was performed over a 30 x 30 km area with 0.25 km grid spacing by using the GRAV3D software from UBC-GIF [17]. No noise was added to the synthetic data in order to simplify the characterization of the results. Figure 1 shows a perspective view of the synthetic models with their associated gravity anomaly maps and profiles. The negative gravity anomaly with about -50 mGal maximum amplitude shows fairly clear boundaries of the anomalous zone.

The SVDs of the gravity data are more representative of the anomalous source's geometry. Its boundaries are better delineated by SVD with oscillations between minimum and maximum (extremum) values across each density contrast transition (Figure 2). On the SVD maps, the 'polarity' of the anomaly can still be identified, i.e. the low density in the central part relative to its surroundings,

although it involves very small differences of the SVD value around zero. The West-East profiles of the SVD crossing the center of the anomalous zone shown in Figure 2 confirm Bott's simple criteria [15,16], as stated before.

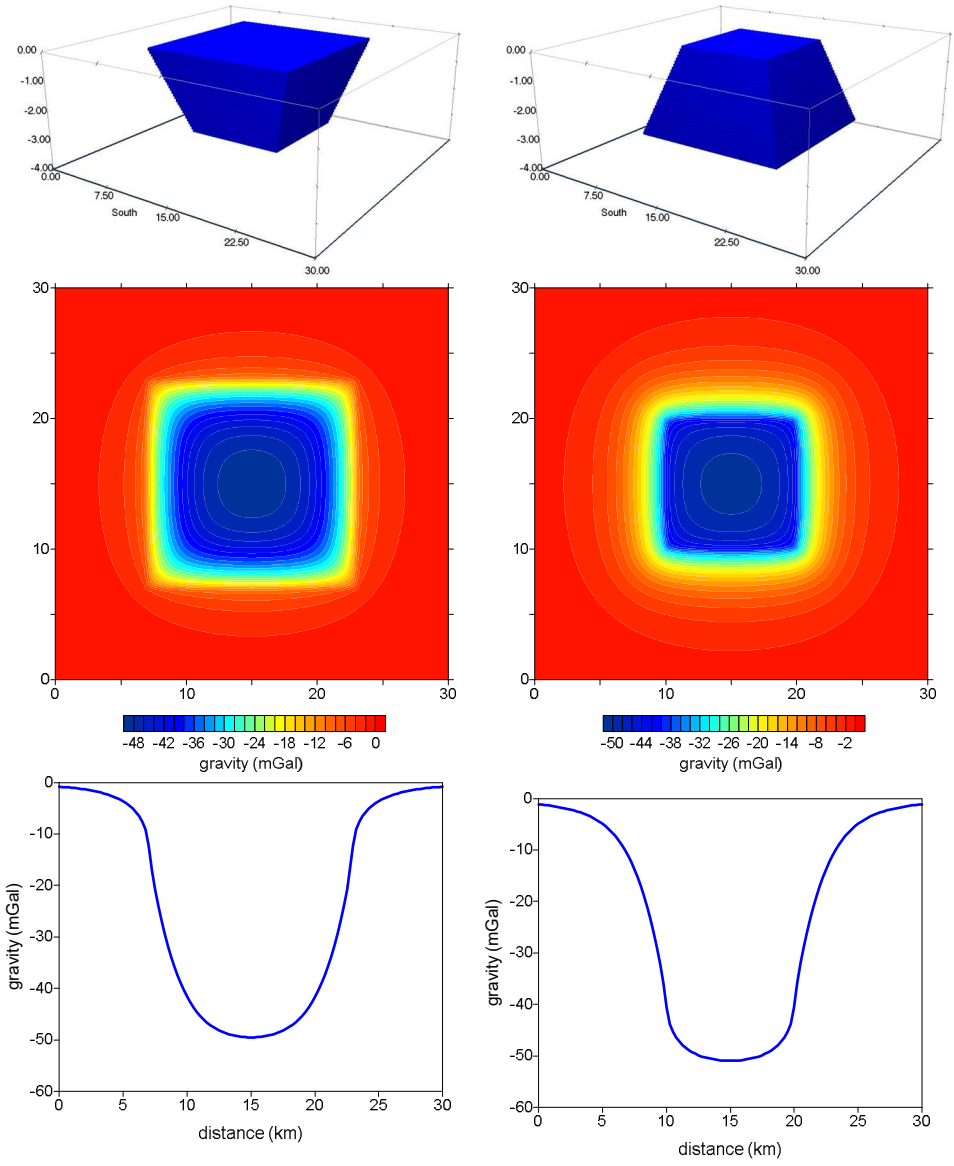

Figure 1 From top to bottom: perspective view of the synthetic model, gravity anomaly map and gravity anomaly profile crossing the central part of the area, for basin (a) and pluton (b). All length units are in kilometers.

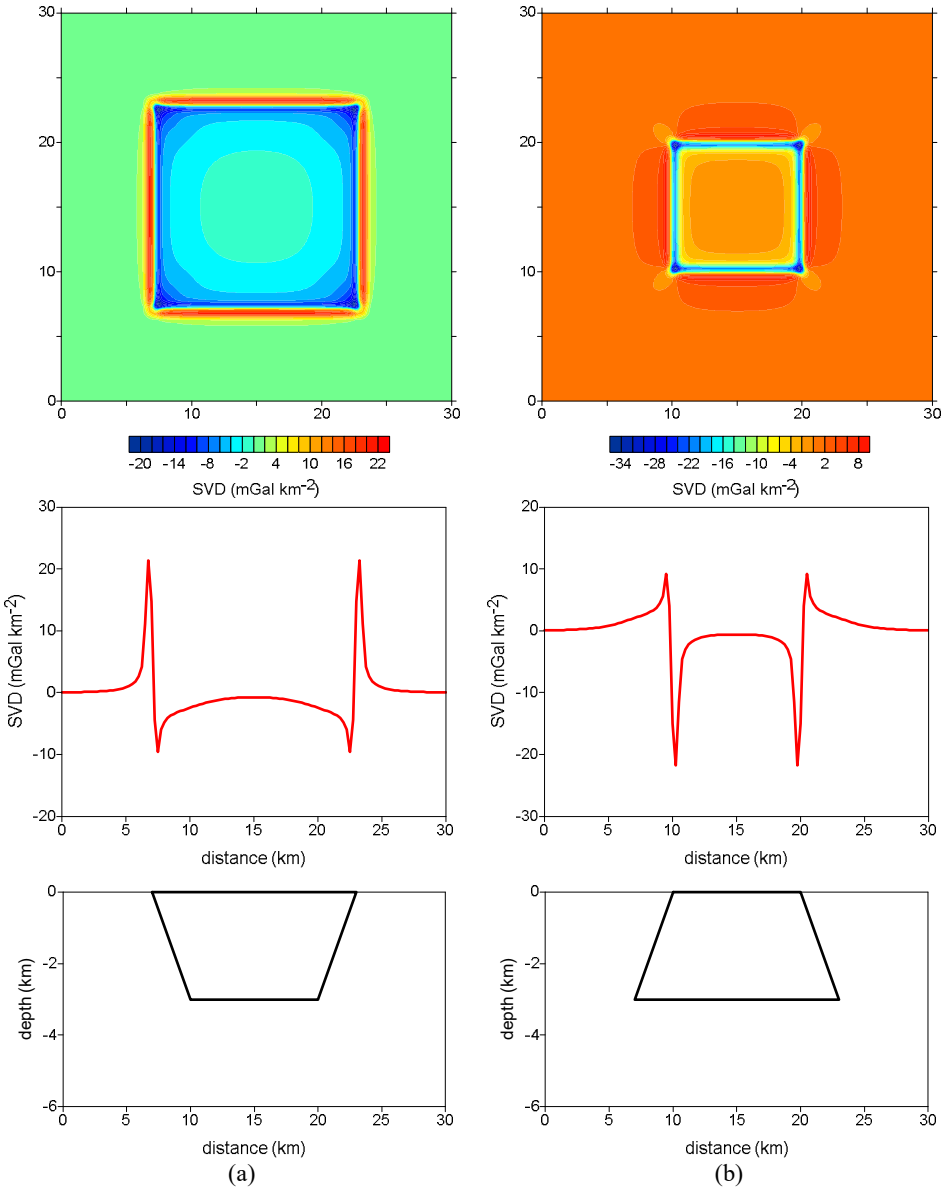

Figure 2 From top to bottom: SVD map, SVD profile and synthetic model cross-section traversing the center of the anomalous zone, for basin (a) and pluton (b). All length units are in kilometers.

The adoption of Bott's criteria by many Indonesian practitioners and academics (lecturers and their students) to determine fault type from SVD is misleading [e.g. 9-11]. They consider only one side of the features (i.e. half-basin or half-

pluton) and use the relative magnitude of g''_{max} and g''_{min} to determine the fault type separating the density contrast. More particularly, if $|g''_{max}|$ is greater than $|g''_{min}|$ then the gravity anomaly is due to a normal fault dipping toward the low anomaly part, as if it is a half-graben. Conversely, if $|g''_{max}|$ is smaller than $|g''_{min}|$ then the gravity anomaly is associated with a reverse fault going upward to the low anomaly part, as if it is a half-horst.

We then considered synthetic models of a basin and a pluton similar to the previous case, but with high-density anomalous sources (density contrast +0.5 gr/cm^3). The SVDs along the profiles crossing the center of the anomalous zone (not shown) are exactly mirror images of the SVD profiles for a negative density contrast (see Figure 2, central panel) with respect to the horizontal axis, i.e. zero SVD. For the left or right part of the profiles for both high and low density anomalies there are consistencies of relationship between relative SVD magnitude and density transition (from higher to lower density and vice versa) along with a dip in the density contrast's interface.

A schematic summary of the consistencies described above is shown in Figure 3. For the same density transition (for example from low to high) the SVD profile is flipped horizontally when the interface's dip is inverted, as can be seen in Figures 3a and 3b and Figures 3c and 3d. For the same interface's dip, the SVD profile is flipped vertically when the density transition is interchanged (see Figures 3a and 3d and Figures 3b and 3c). In the latter case, the SVD profile is mirrored with respect to the horizontal line of zero SVD. These kinds of density transitions and their slope orientation cannot be used to determine the fault type. Therefore, the extension of Bott's criteria to determine the fault type is erroneous since the definition of a fault in geology is very precise [e.g. 18] and it can be determined only from field observation of displaced rock units.

Lack of fundamental conceptual understanding and lack of effort in finding freely available computer resources [14] lead to apparent difficulties in calculating the SVD in 2D as an SVD map. The latter motivates the use of approximations, where the SVD is calculated only along a profile using Eq. (2). This type of approximation is also intended to make use of Bott's criteria [16,17] but with the intention to determine the fault type [9-11].

When the model is relatively simple with a large dimension (elongated) along the y-axis, the SVD approximation along the x-axis is still valid, as shown in Figure 4 for the same synthetic models as before. The SVD profiles would be identical to those from the calculation without approximation (Figure 2). However, the magnitude of the SVD is relatively small, i.e. between ±20 mGal/km^2 in our synthetic case. The unit in mGal/m^2 as in [9-11] further leads to very small SVD values. Fundamental oscillations of the SVD across

boundaries of simple structures may be lost for complex subsurface structures due to overlapping anomalies. The use of approximations with mostly sparse data as in a real gravity survey may result in an erroneous interpretation.

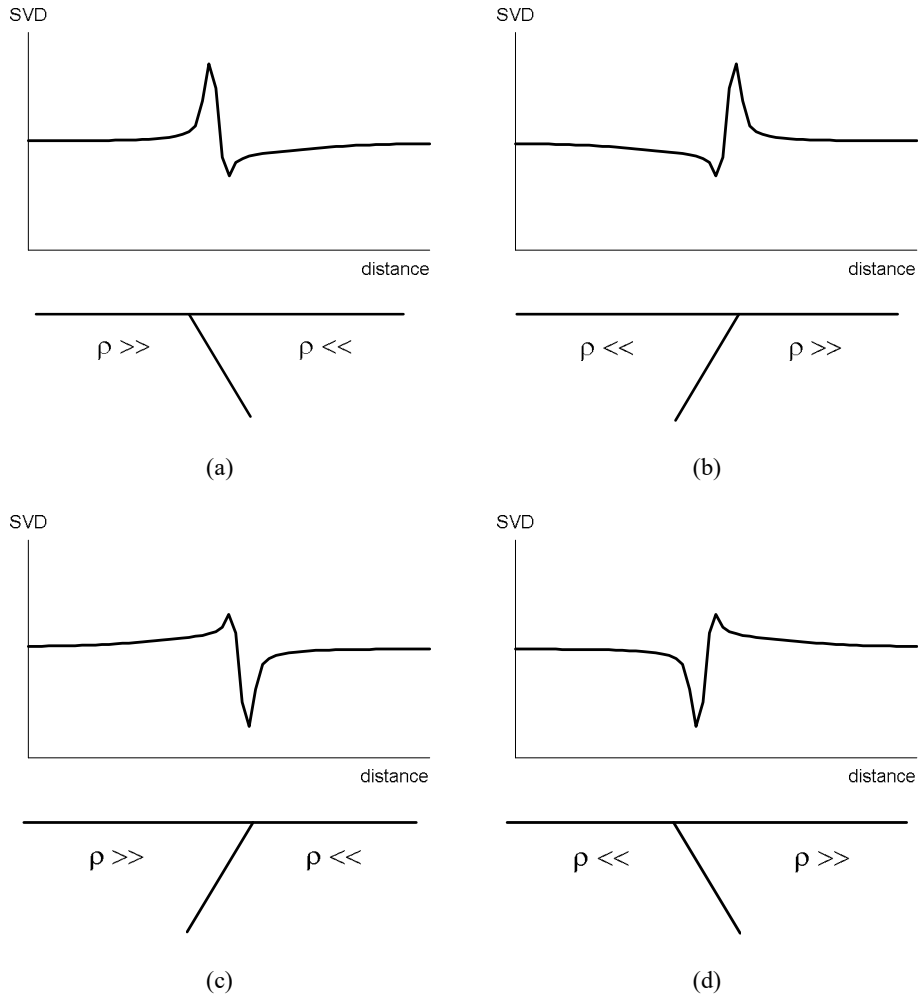

Figure 3 Schematic relationship between the interface's dip of density contrast or density transition and the SVD profile. See the text for details.

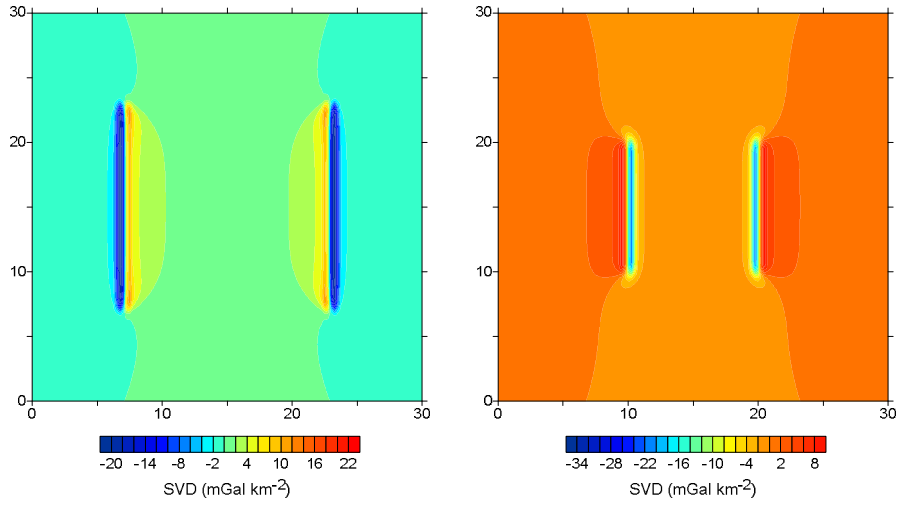

(a) (b)

Figure 4 SVD map obtained from approximation using the second horizontal derivative of synthetic models for a basin (a) and a pluton (b). The color scales are identical to those used in Figure 2 to emphasize their similarity. All length units are in kilometers.

4 SVD of Overlapping Anomalies

To illustrate the complexity of gravity gradients in more realistic cases, we performed a similar exercise with a different 3D synthetic model. We used a two-block model representing a basin with vertical slopes and different depths (1.5 km and 3 km) with a density contrast of -0.5 gr/cm^3. All other calculation parameters were the same as in the previous synthetic model.

The gravity anomaly is asymmetrical with similar maximum magnitude as the anomaly in the previous single-body synthetic model, i.e. about -48 mGal, since the maximum depth of the basin is also 3 km. Only the outermost edges of the basin can be identified from the SVD. Compared to the results from the previous synthetic model, the symmetrical SVD across the outer edges of the anomalous source is related to the vertical rather than the gradual contact of the density. The intra-basin depth variation is almost indistinguishable due to overlapping anomalies (see Figure 5). This example demonstrates difficulties in the use of SVD for anomalous source delineation in a more complex situation. In Figure 5 we also plotted the SVD profile along with its approximation using the second horizontal derivative. Both curves are almost identical such that they appear to be one single curve.

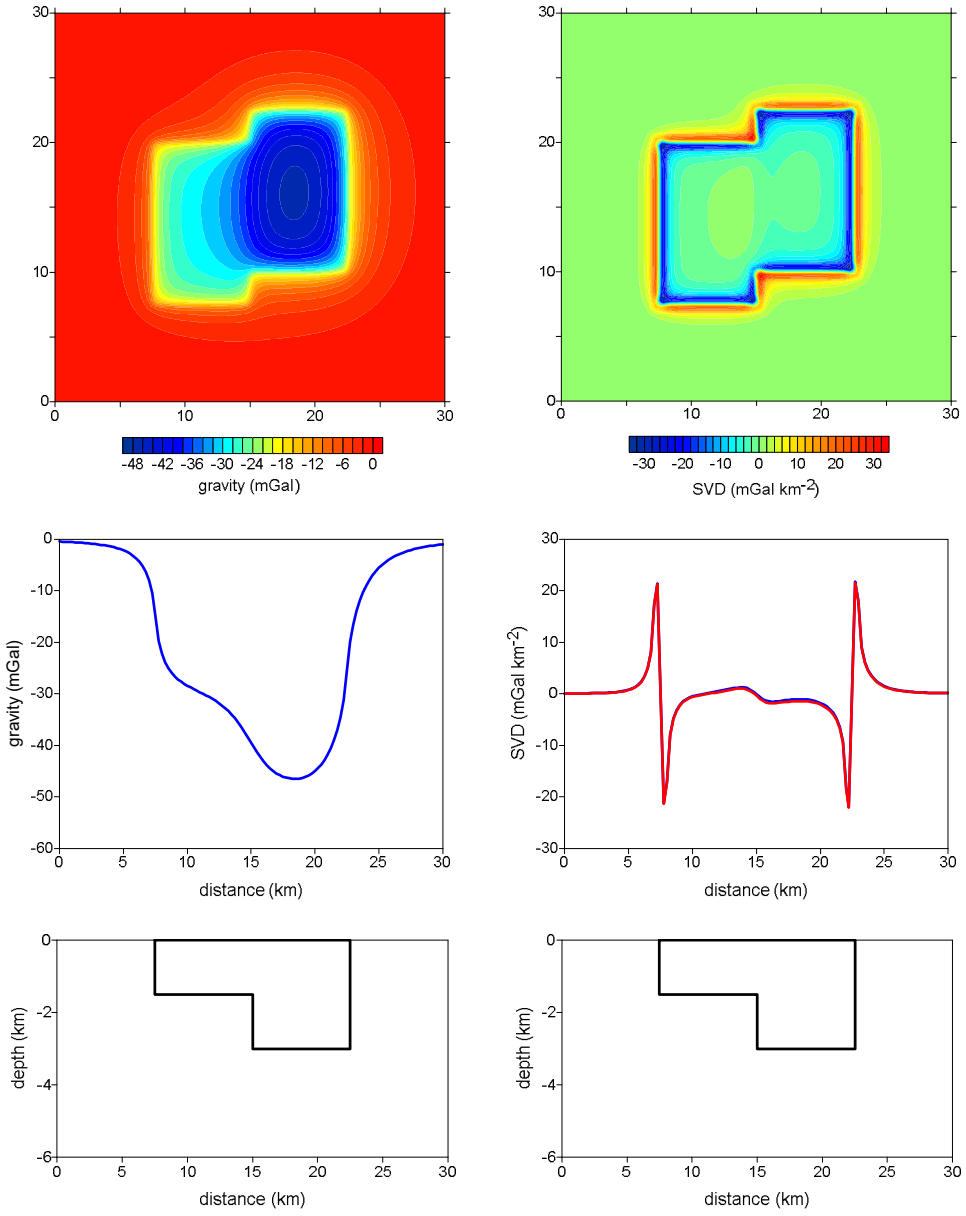

(a) (b)

Figure 5 Results from synthetic model with different basin depths, from top to bottom: anomaly map, anomaly profile and synthetic model cross-section traversing the center of the anomalous zone for gravity anomaly (a) and SVD (b). All length units are in kilometers. See the text for details.

5 Example with Field Data

The Bouguer anomaly maps of several quadrangles from the western part of West Java published by the Geological Survey of Indonesia [19] were digitized and a grid spacing of 1 x 1 km was applied (Figure 6a). We applied SVD analysis to the gridded data using a spatial domain calculation to obtain an SVD map. Contrary to SVD analysis from a simple model – hence with a simple gravity anomaly – the SVD map and profiles of real gravity are very difficult to interpret due to the complexity of the geology, i.e. the anomalous sources. The latter leads to complex and overlapping gravity anomalies. In addition, the high-frequency content of the anomalies is enhanced, although we used the spatial domain calculation to minimize noise amplification commonly encountered in wave-number domain processing (see Figure 6b).

Performing analysis and interpretation from the SVD for boundary delineation and to determine the associated type of fault would be very difficult or even prohibitive due to the overlapping anomalies. In the present case, the SVD magnitude is very small, i.e. maximum ±7.0 mgal/km^2 with certainly smaller values dominating most of the area. In addition to complicated resultant anomalies, overlapping anomalies tend to cancel each other out, leading to smaller SVD amplitude. Therefore, SVD analysis is only useful for relatively simple structures or at most for a relatively isolated anomaly with well-defined prior information on the geology. Furthermore, poor data coverage, as in most cited references [e.g. 9-11], tends to over-simplify the structures present in the area of study.

Delineation of basin boundaries from gravity data would be more appropriate by using spectral-based filtering [20,21]. If information on spatial frequency content of the data is obtained from spectral analysis, certain frequency ranges can be enhanced or attenuated using a filter. Low-frequency (i.e. regional) data are filtered out, thus enhancing more local or shallower anomaly features (e.g. basin). From the radially averaged spectrum in Figure 6c, the wave-number cut-off for regional structures is around 0.02 km^{-1} corresponding to a 50-km wavelength. We consider that the residual anomaly presented in Figure 6d is more informative than that from SVD and agrees well with the geology of the area. Further geological interpretation is beyond the scope of this paper since this case only serves as an alternative example for SVD analysis.

6 Concluding Remarks

Lack of awareness of the fundamental concepts and limited capability in implementing the calculation of gravity gradients, in particular the SVD, have led to pragmatic but inappropriate practices. Therefore, it is very important to

definitively correct this misconception. The relative magnitude of the SVD can only be used to determine the density change and the dip orientation of an interface. Those characteristics of the density contrast, and hence the SVD, cannot be associated unambiguously with the fault type.

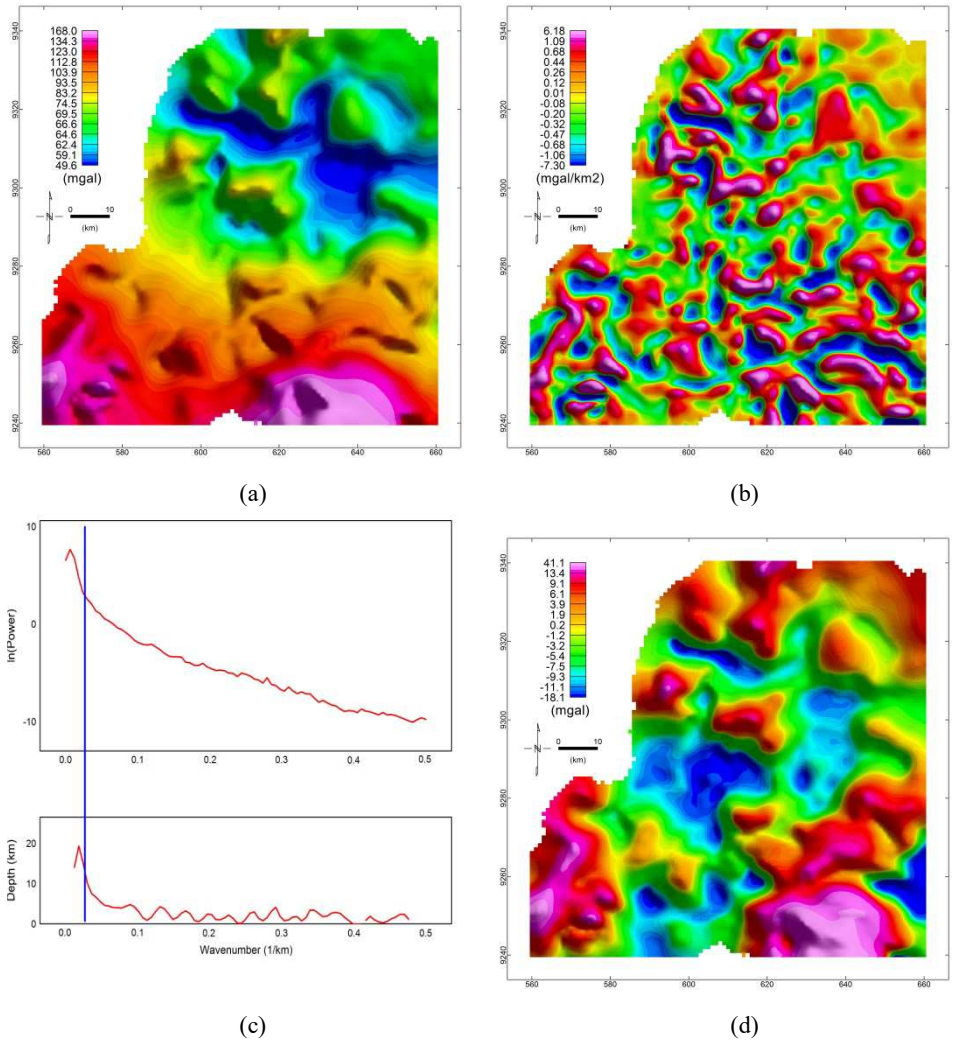

Figure 6 (a) Bouguer anomaly map of the western part of West Java, (b) SVD map obtained using spatial domain calculation, (c) radially averaged spectrum to determine the cut-off wave-number, (d) residual anomaly after filtering the Bouguer anomaly with a cut-off wavelength of 50 km.

This paper does not intend to downgrade the utility of the SVD analysis of gravity data. As long as the computational algorithm is correct, the interpretation is appropriate and its limitations are considered, the information gained from SVD can be valuable in exploration programs. Nevertheless, the use of SVD analysis should be limited to relatively simple structures for qualitative interpretation only. Our results with field data showed that wave-number filtering is relatively superior to SVD and other techniques based on gradients (e.g. horizontal gradient magnitude or total gradient for basin delineation).

Spectral-based analysis has been the standard technique for advanced gravity and magnetic data processing in research and industry for a long time. It should also become the standard in education. As for limited availability of computational tools, this situation can be considered an opportunity to encourage the development of computer programs or code to perform such data analysis. There are also possibilities to use freely available computer programs or even software applications that are available on the Internet, e.g. from academic or research institution web pages, computer and geosciences related journals, and other repositories [14]. Such efforts open almost unlimited possibilities to support teaching materials, topics for undergraduate final projects or even graduate theses.

Acknowledgements

The authors acknowledge the support from P3MI ITB for the Applied and Exploration Geophysics Research Group in 2017.

References

[1] LaFehr, T.R. & Nabighian, M.N., *Fundamentals of Gravity Exploration*, Geophysical Monograph Series 17, SEG, 2012.
[2] Fairhead, J.D., *Advances in Gravity and Magnetic Processing and Interpretation*, EAGE Publications, 2015.
[3] Roy, L., Agarwal, B.N.P. & Shaw, R.K., *A New Concept in Euler Deconvolution of Isolated Gravity Anomalies*, Geophysical Prospecting, **48**(3), pp. 559-575, 2000.
[4] Ma, G., *Combination of Horizontal Gradient Ratio and Euler Methods for the Interpretation of Potential Field Data*, Geophysics, **78**(5), pp. J53-J60, 2013.
[5] Blakely, R.J., *Potential Theory in Gravity and Magnetic Applications*, Cambridge University Press, 1996.
[6] Elkins, T.A., *The Second Derivative Method of Gravity Interpretation*, Geophysics, **16**(1), pp. 29-50, 1951.

[7] Baranov, V., *Potential Fields and their Transformations in Applied Geophysics*, Geoexploration Monograph 6, Geopublication Associates, 1975.
[8] Widianto, E., *Determination of Basement Structure Configuration and Basin Types Using Gravity Data and its Implication for Oil and Gas Exploration Target in Java*, Doctoral thesis, Institut Teknologi Bandung, 2008. (Text in Indonesian with English abstract)
[9] Sarkowi, M., *Identification of Structures in Ulubelu Geothermal Field Based on SVD Data Analysis of Bouguer Anomaly* (in Indonesian with English abstract), Jurnal Sains MIPA, **16**(2), pp. 111-118, 2010.
[10] Hartati, A., *Identification of Fault Structure Based on Derivative Analysis of Gravity in Celebes Island*, Undergraduate Final Project, Universitas Indonesia, 2012. (Text in Indonesian with English abstract)
[11] Ali, Y.H., Azimi, A. & Wulandari, A., *Mapping of Nusa Laut Fault Based on Nusa Laut August-September 2015 Earthquake Hypocenters and Gravity Data*, Proceedings of National Seminar on Physics and its Applications, Universitas Padjadjaran, pp. FB11-FB18, 2015. (Text in Indonesian with English abstract)
[12] Mickus, K.L. & Hinojosa, J.H., *The Complete Gravity Gradient Tensor derived from the Vertical Component of Gravity: A Fourier Transform Technique*, Journal of Applied Geophysics, **46**(3), pp. 156-176, 2001.
[13] Grandis, H. & Dahrin, D., *Full Tensor Gradient of Simulated Gravity Data for Prospect Scale Delineation*, Journal of Mathematics and Fundamental Sciences, **46**, pp. 107-124, 2014.
[14] Grandis, H. & Dahrin, D., *The Utility of Free Software for Gravity and Magnetic Advanced Data Processing*, IOP Conf. Series: Earth and Environmental Science, **62**(012046), 2017.
[15] Bott, M.P.H., *A Simple Criterion for Interpreting Negative Gravity Anomalies*, Geophysics, **27**(3), pp. 376-381, 1962.
[16] Reynolds, J.M., *An Introduction to Applied and Environmental Geophysics*, 2nd Edition, Wiley-Blackwell, 2011.
[17] Li, Y. & Oldenburg, D.W., *3D Inversion of Gravity Data*, Geophysics, **63**(1), pp. 109-119, 1998.
[18] Spooner, A.M., *Geology for Dummies*, John Wiley & Son, 2011.
[19] Untung, M. & Sato, Y., *Gravity and Geological Studies in Jawa, Indonesia*, Geological Survey of Indonesia & Geological Survey of Japan, 1978.
[20] Buttkus, B., *Spectral Analysis and Filter Theory in Applied Geophysics*, Springer, 2000.
[21] Sanchez-Rojas, J., *New Bouguer Gravity Maps of Venezuela: Representation and Analysis of Free-Air and Bouguer Anomalies with Emphasis on Spectral Analyses and Elastic Thickness,* International Journal of Geophysics*,* Article ID 731545, 2012.